◆ Human Brain Mapping 37:1759–1769 (2016) ◆

Development and Aging of Superficial White Matter Myelin From Young Adulthood to Old Age: Mapping by Vertex-Based Surface Statistics (VBSS)

Minjie Wu,[1] Anand Kumar,[1] and Shaolin Yang[1,2,3]*

[1]*Department of Psychiatry, University of Illinois at Chicago, Chicago, Illinois*
[2]*Department of Radiology, University of Illinois at Chicago, Chicago, Illinois*
[3]*Department of Bioengineering, University of Illinois at Chicago, Chicago, Illinois*

Abstract: Superficial white matter (SWM) lies immediately beneath cortical gray matter and consists primarily of short association fibers. The characteristics of SWM and its development and aging were seldom examined in the literature and warrant further investigation. Magnetization transfer imaging is sensitive to myelin changes in the white matter. Using an innovative multimodal imaging analysis approach, vertex-based surface statistics (VBSS), the current study vertexwise mapped age-related changes of magnetization transfer ratio (MTR) in SWM from young adulthood to old age (30–85 years, $N = 66$). Results demonstrated regionally selective and temporally heterochronologic changes of SWM MTR with age, including (1) inverted U-shaped trajectories of SWM MTR in the rostral middle frontal, medial temporal, and temporoparietal regions, suggesting continuing myelination and protracted maturation till age 40–50 years and accelerating demyelination at age 60 and beyond, (2) linear decline of SWM MTR in the middle and superior temporal, and pericalcarine areas, indicating early maturation and less acceleration in age-related degeneration, and (3) no significant changes of SWM MTR in the primary motor, somatosensory and auditory regions, suggesting resistance to age-related deterioration. We did not observe similar patterns of changes in cortical thickness in our sample, suggesting the observed SWM MTR changes are not due to cortical atrophy. *Hum Brain Mapp 37:1759–1769, 2016.*

Key words: white matter; development and aging; myelin; cortical thickness; magnetization transfer

Additional Supporting Information may be found in the online version of this article.

Contract grant sponsor: National Institutes of Health (NIH); Contract grant numbers: R01-MH63764 and R01-MH73989; Contract grant sponsor: National Center for Advancing Translational Sciences of NIH; Contract grant number: KL2TR000048; Contract grant sponsor: Creative and Novel Ideas in HIV Research (CNIHR) Program through a supplement to the University of Alabama at Birmingham (UAB) Center For AIDS Research funding. This funding was made possible by collaborative efforts of the Office of AIDS Research, the National Institute of Allergy and Infectious Diseases, and the International AIDS Society; Contract grant number: P30 AI027767.

All the authors have no conflict of interest to disclose.

*Correspondence to: Shaolin Yang, Departments of Psychiatry, Radiology, and Bioengineering, University of Illinois at Chicago, 1601 W. Taylor St., Suite 512, Chicago, IL 60612. E-mail: syang@psych.uic.edu

Received for publication 26 April 2015; Revised 7 January 2016; Accepted 26 January 2016.

DOI: 10.1002/hbm.23134

Published online 9 March 2016 in Wiley Online Library (wileyonlinelibrary.com).

INTRODUCTION

Superficial white matter (SWM) lies immediately beneath the cortical mantle and consists primarily of short association fibers, called the U-fibers of Meynert [1872], which make up the majority of corticocortical white matter pathways in the human brain. After leaving the cortex, U-fibers travel tangentially along the cortical folding within SWM, and re-enter the adjacent cortex at a distance up to 30 mm, connecting neighboring gyri. Within the central nervous system, U-fibers are among the slowest myelinating fibers and the myelination process may extend into the fourth decade of life [Barkovich, 2000; Schüz et al., 2006; Maricich et al., 2007; Reiser et al., 2008], which makes the U-fibers and SWM vulnerable to cumulative developmental insults. Understanding nondisease-related changes in SWM during normal development and aging can inform pathological changes associated with age-related neurodegenerative disorders such as Alzheimer's disease. Microstructural changes in SWM during normal development and aging have seldom been systematically examined across the entire cortical mantle, except for recent diffusion tensor imaging (DTI)-based studies probing fiber coherence in SWM [Tamnes et al., 2010; Phillips et al., 2013; Wu et al., 2014]. However, to date no studies have evaluated the accompanied biophysical changes of the macromolecular protein pools (i.e., myelin) in SWM from young adulthood to old age, which warrants further investigation.

Magnetic resonance imaging (MRI) has been used to study macro- and microstructural changes in white matter (WM) from healthy young adulthood to old age. White matter volume shows a nonlinear decline with age in younger adults, and reaches a plateau in middle age before progressing precipitously in older adults [Jernigan et al., 2001; Raz et al., 2005]. White matter hyperintensities (WMH), areas with higher intensity than normal-appearing WM on T_2-weighted images, are also common and increase with age in normal elderly adults [Ylikoski et al., 1995; Longstreth et al., 1996]. White matter hyperintensities are believed to be of ischemic origin except for lesions around the borders of the ventricles (i.e., periventricular WMH) [Fazekas et al., 1993; Spilt et al., 2006; Kim et al., 2008]. With the advent of DTI, it became possible to noninvasively probe age-related WM changes at a microscopic level. For deep white matter tracts, age-dependent decrease in fractional anisotropy (FA) is more prominent in association tracts (i.e., the superior longitudinal fascicle, inferior fronto-occipital fascicle, and inferior longitudinal fascicle) than projection tracts [Stadlbauer et al., 2008]. Specifically, age-related deterioration is greater in the anterior than posterior segments of association tracts [Davis et al., 2009]. In SWM, age-related decrease of FA is more pronounced in the prefrontal white matter, relative to parietal regions [Sullivan et al., 2001; Phillips et al., 2013], whereas increase in radial diffusivity (RD) is observed in widespread SWM regions [Phillips et al., 2013].

Magnetization transfer (MT) imaging has been used to examine developmental and pathological changes in the macromolecular protein pools of brain tissues, through indirect measurement of protons bound to macromolecules [Chen et al., 2008; Kumar et al., 2009]. Compared to free protons in tissue water, protons bound to macromolecules (e.g., myelin in WM and cell membrane proteins and phospholipids in gray matter [GM]) are less mobile and usually undetectable by conventional MRI, as bound protons have very short T_2 relaxation time and MR signal from bound protons decays rapidly to the noise level before data readout [Wolff and Balaban, 1989; Henkelman et al., 2001; Cercignani and Alexander, 2006]. In MT imaging, an off-resonance prepulse is applied to selectively saturate the bound protons, and magnetization is then transferred from the saturated bound protons to free protons through exchange mechanisms such as chemical exchange and direct dipolar coupling. Magnetization transfer leads to decreased MR signal from the free protons. The contrast between MT images with and without the saturation prepulse indirectly measures the bound protons and accordingly informs the biophysical integrity of macromolecular protein pools in brain tissue [Mehta et al., 1996]. Within WM, MT effects are dominantly contributed by the macromolecular protein pools associated with myelin [Stanisz et al., 1999]. Therefore, magnetization transfer ratio (MTR), a contrast index derived from MT images, can probe changes in macromolecular protein pools and provide specific information on the myelin status in WM.

Previous studies on age-related MTR changes in WM have reported inconsistent findings that the MTR either remained relatively stable [Mehta et al., 1995], or increased [Armstrong et al., 2004], or decreased [Hofman et al., 1999; Ge et al., 2002; Fazekas et al., 2005] from healthy young adulthood to old age. In these studies, linear age effects were evaluated on regional MTR with region of interest (ROI)-based methods [Mehta et al., 1995; Armstrong et al., 2004; Fazekas et al., 2005] or on global MTR using histogram-based approaches [Hofman et al., 1999; Ge et al., 2002]. While providing valuable insights into the WM development and aging, these studies lacked fine spatial details in probing MTR changes and did not model nonlinear age effects, which might jointly lead to the aforementioned inconsistency. Therefore, MT-based studies with finer spatial scales and nonlinear age models are needed to clarify the changing patterns of macromolecular protein pools (i.e., myelin) in SWM from young adulthood to old age.

In the current study, we developed an innovative multimodal image analysis approach, vertex-based surface statistics (VBSS), to automatically map individual SWM MTR onto a common surface and vertexwise characterize the effects of age on SWM MTR across the entire cortex in healthy adults from 30 to 85 years of age. Consistent with previous findings on regional WM variations in DTI-derived indices [Tamnes et al., 2010; Phillips et al., 2013;

Wu et al., 2014], we hypothesized that SWM would present regionally selective and temporally heterochronologic changes in MTR from young adulthood to old age.

MATERIALS AND METHODS

Subjects

The data of this study were collected at the University of Illinois at Chicago (UIC), Department of Psychiatry. Participants selected for this study were all healthy volunteers with age of 30 and older, and were recruited from the greater Chicago area through flyers and local advertisements. Exclusion criteria included: current or past history of neurological and psychiatric disorders (i.e., dementia, stroke, seizure, transient ischemic attack, and depression), learning disability or attention deficit hyperactivity disorder, significant head trauma, active psychotropic medication, current or past history of substance dependence, and Type 1 or Type 2 diabetes.

The subject sample consisted of 66 healthy adults in the age range of 30–85 years, of which 36 participants were females and all were right handed. The sample had a mean age of 60.22 ± 14.51 years (mean $\pm$ standard deviation), mean full scale IQ at 106.80 ± 12.20, mean years of education at 16.03 ± 3.00, mean Cumulative Illness Rating Scale (CIRS) at 3.80 ± 2.52, mean Mini-Mental Status Examination (MMSE) score at 29.20 ± 0.95, mean Hamilton Depression Rating Scale (HDRS) score at 1.00 ± 1.38, and mean hemoglobin A1c (HbA1c) level at $5.62 \pm 0.34\%$ (38 ± 3.7 mmol/mol). The study was approved by the UIC Institutional Review Board and written informed consent was obtained from all participants.

MRI Data Acquisition

MRI scans were performed on a Philips Achieva 3T scanner (Philips Medical Systems, Best, the Netherlands) with an 8-element phased-array (Philips SENSE-Head-8) coil. Participants were equipped with soft ear plugs, positioned comfortably in the head coil using custom-made foam pads to minimize head motion, and instructed to remain still. The MT images were acquired using a three-dimensional (3D) spoiled gradient-echo sequence with multishot echo-planar imaging (EPI) readout: TR/TE = 64/15 ms, flip angle = 9°, FOV = 24 cm, 67 axial slices, slice thickness/gap = 2.2 mm/no gap, EPI factor = 7, reconstructed voxel size = $0.83 \times 0.83 \times 2.2$ mm^3, P reduction factor = 2, with a nonselective five-lobed Sinc-Gauss off-resonance MT prepulse ($B_1/\Delta f/\text{dur} = 10.5$ μT/1.1 kHz/24.5 ms) [Smith et al., 2006]. The image slices were prescribed axially, parallel to the anterior commissure–posterior commissure plane. Prior to the MT scan, a high resolution 3D T_1-weighted (T1w) magnetization prepared rapid acquisition gradient echo (MPRAGE) image was acquired: TR/TE = 8.4/3.9 ms, flip angle = 8°, FOV = 24 cm, 134 axial slices/no gap, reconstructed voxel size = $0.83 \times 0.83 \times 1.1$ mm^3, for intersubject cortical spatial normalization and registration.

Image Processing

The proposed VBSS analysis pipeline of T1w and MT images is summarized in Figure 1. For each subject, FreeSurfer (https://surfer.nmr.mgh.harvard.edu/) was used on the T1w image for automated intersubject cortical spatial normalization and for cortical thickness estimation, based on individual's cortical folding patterns. Customized manual interventions were applied when the automated processing stream failed. Individual T1w image was first linearly registered to the Talairach space [Talairach and Tournoux, 1988; Collins et al., 1994]. This transformation result was visually checked and was manually reoriented and/or scaled when necessary. Next, the intensity variation in WM was used to estimate the bias field from B_1 inhomogeneity, which was used for intensity inhomogeneity correction on the T1w image. Skull stripping was performed to remove the nonbrain tissue using a deformable model, and WM was segmented based on intensity and neighbor constraints. The brain mask was also visually inspected and input parameters were adjusted to improve skull stripping. Control points were manually added within the WM boundary to avoid erroneous WM segmentation. Next, the white surface (gray–white boundary) was generated by tilting the outside of the WM and refined by following the intensity gradient between GM and WM. The pial surface was estimated by nudging the WM surface to follow the intensity gradients between GM and CSF. Cortical surface of each hemisphere was inflated, warped, and normalized to the standard average spherical atlas based on cortical folding patterns (individual T1w surface → template surface) [Dale et al., 1999; Fischl et al., 1999a, 1999b].

For each subject, the MT images with (M_s) and without the MT prepulse (M_0) were coregistered for motion correction, and the MTR image was voxelwise calculated using the following formula: $\text{MTR} = (M_0 - M_s)/M_0$. The M_s image was further coregistered with the T1w image. Skull stripping was performed on both images (M_s and T1w) prior to coregistration for improved accuracy. With the M_s → T1w intrasubject transformation, SWM MTR was averaged and projected onto individual WM surface. Specifically, to reduce partial volume effects, SWM MTR at each vertex was determined by averaging the MTR values of SWM sampled along the WM surface normal from 1 mm to up to 5 mm of distance to the WM surface. The SWM MTR surface map in individual T1w surface space was further projected onto the common template surface using the T1w → template surface transformation. Surface-based smoothing with a 10-mm FWHM Gaussian kernel was then applied to the warped SWM MTR surface maps. The proposed multimodal image analysis method, called

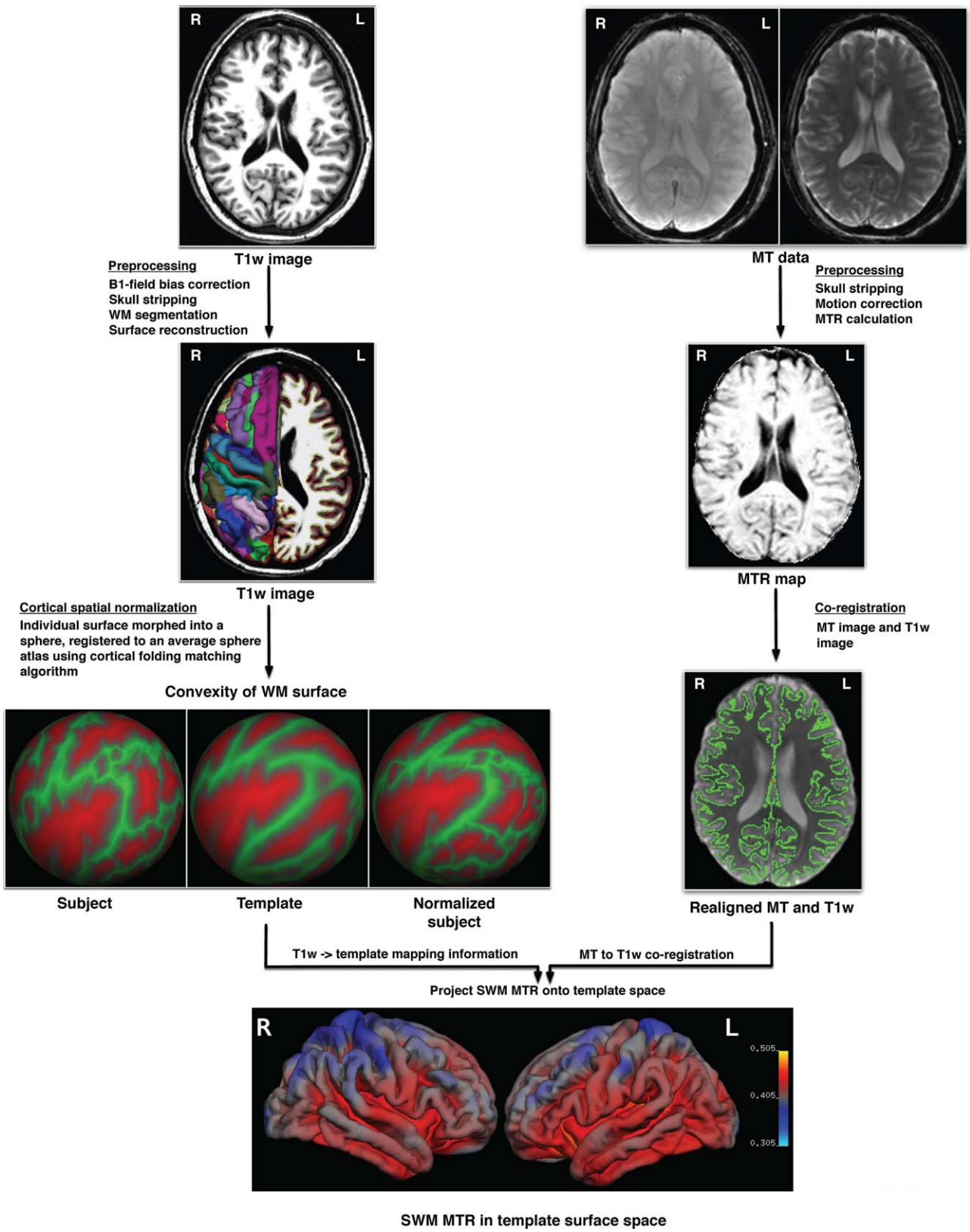

Figure 1.

Analysis pipeline of vertex-based surface statistics (VBSS) (L = left; R = right). [Color figure can be viewed in the online issue, which is available at wileyonlinelibrary.com.]

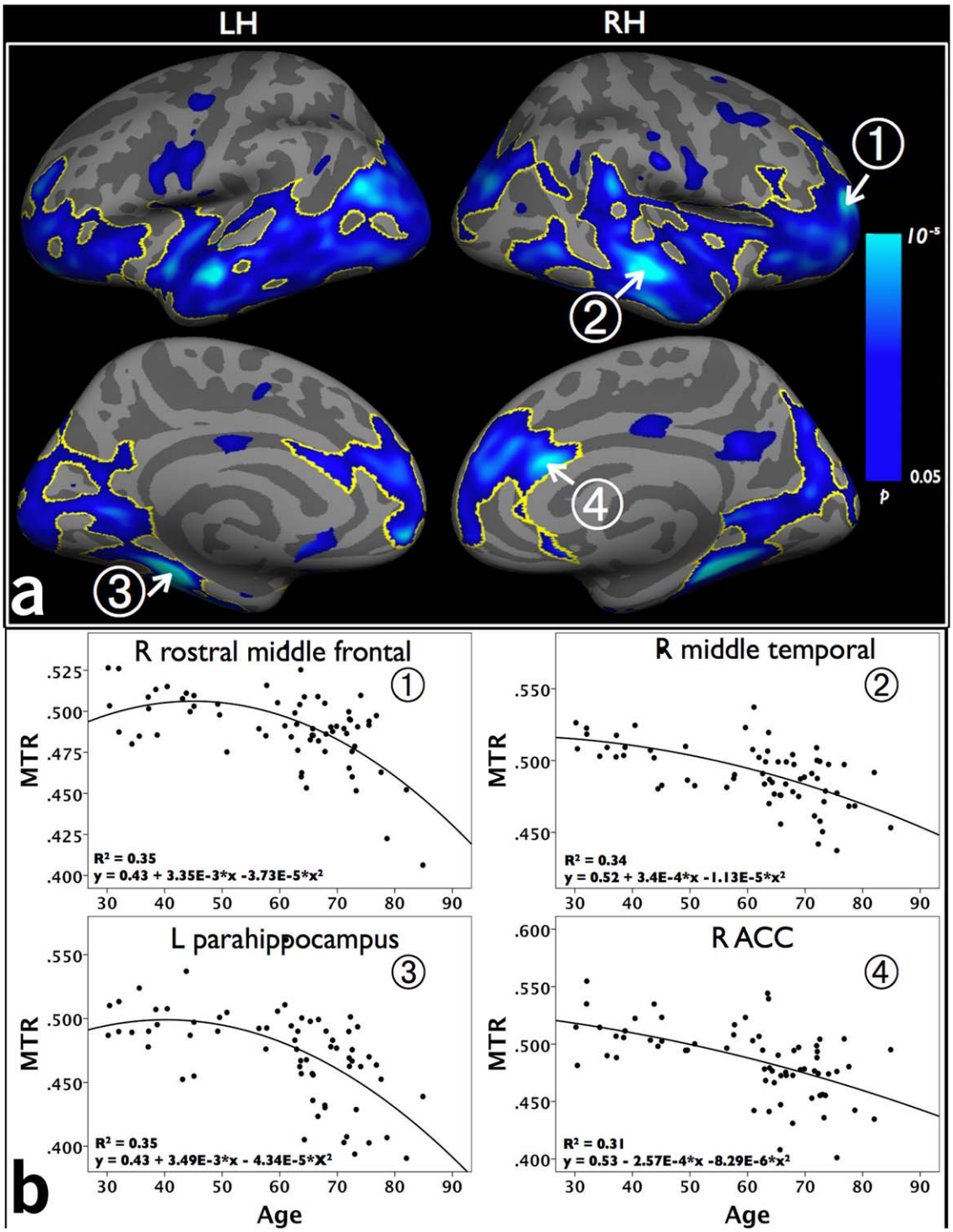

Figure 2.

(a) Significant age-associated changes of SWM MTR from young adulthood to old age (age range: 30–85 years). The gold-edged clusters outline the SWM regions that survived multiple comparisons with a corrected $P < 0.0001$. (LH = left hemisphere; RH = right hemisphere). (b) Scatterplots of SWM MTR (y-axis) and age (x-axis) at four representative vertices as marked in (a): (1) right rostral middle frontal, (2) right middle temporal, (3) left parahippocampus, and (4) right anterior cingulate cortex (ACC) (L = left; R = right). Depending on the "goodness of fit" r^2, the curves in the graphs represent linear or quadratic line fittings of SWM MTR and age. [Color figure can be viewed in the online issue, which is available at wileyonlinelibrary.com.]

"vertex-based surface statistics (VBSS)," maps SWM MTR images from individual space onto the common template surface and facilitates vertexwise cross-subject statistical comparisons of SWM MTR across the cortical surface.

Statistical Analysis

General linear model (GLM) analyses were performed to test the effects of gender and age on SWM MTR and cortical thickness at each vertex, with linear and quadratic terms of age (age and age^2) as continuous covariates. A cluster-size threshold was estimated with Monte Carlo simulation (10,000 iterations of simulation) and was used to correct for multiple comparisons [Hagler et al., 2006].

RESULTS

Preliminary Analyses

The GLM analyses with age and gender as between-subject contrasts yielded no significant main effect of gender or age × gender interaction (corrected P's < 0.05). There were no significant gender-related variations in SWM MTR or gender-related differences in the rates of SWM MTR change with age. Therefore, male and female participants are combined in the following GLM analyses of age effects.

Age Effects on SWM MTR

The association between SWM MTR and age was vertexwise evaluated using GLM. The effects of age on SWM MTR were illustrated in Figure 2, in which the gold-edged clusters outlined the SWM areas that survived multiple comparisons (corrected $P < 0.0001$). Significant age-related changes of SWM MTR was observed in widespread SWM regions across all brain lobes: the frontal lobe (bilateral rostral middle frontal, inferior frontal [pars triangularis, pars orbitalis], lateral orbitofrontal, insula, and medial superior frontal), the limbic lobe (bilateral caudal anterior cingulate and parahippocampus), the temporal lobe (bilateral superior and middle temporal, fusiform, and left inferior temporal cortex), the parietal lobe (bilateral angular gyri), and the occipital lobe (bilateral cuneus, pericalcarine, lingual, and lateral occipital cortices). In contrast, there is no significant change of SWM MTR with age in the SWM regions associated with basic motor and sensory functions, such as the primary motor cortex (precentral), somatosensory cortex (postcentral), auditory cortex (Hechl's or transverse temporal gyri), and tertiary heteromodal regions (superior parietal and superior lateral frontal).

To illustrate the heterogeneous patterns of relationship between SWM MTR and age, SWM MTR was plotted by age at 25 SWM vertices in Figure 3. Linear decrease of SWM MTR with age was presented in SWM regions including the frontal lobe (lateral orbitofrontal [Fig. 3b,r], medial superior frontal [Fig. 3j,s]), the limbic lobe (the anterior cingulate [Fig. 3k,u,t]), the temporal lobe (middle and superior temporal [Fig. 3p,e]), and the occipital lobe (pericalcarine [Fig. 3y]). Quadratic age effects on SWM MTR were observed in the frontal lobe (rostral middle frontal [Fig. 3a,q], medial orbitofrontal [Fig. 3l]), the limbic lobe (parahippocampus [Fig. 3i,x]), the parietal lobe (supramarginal [Fig. 3o], the inferior parietal [Fig. 3f,m]), and the occipital lobe (lingual [Fig. 3h]). No significant age-related changes in SWM MTR were observed in the primary motor (precentral, Fig. 3d,n) and somatosensory (postcentral, Fig. 3c), and supplementary motor areas (paracentral, Fig. 3g,v).

Age Effects on Cortical Thickness

Significant cortical thinning with age was found in the primary motor and sensory regions (the precentral gyrus, occipital lobe/calcarine), and association cortices (the right inferior frontal gyrus, right supramarginal, isthmus of cingulate, superior and middle temporal regions) (corrected $P < 0.01$, Supporting Information Fig. 1).

DISCUSSION

To the best of our knowledge, this is the first study to vertexwise characterize the age-related changes in SWM MTR across the entire cortical mantle from healthy young adulthood to old age (30–85 years). We found regionally selective and temporally heterochronologic changes of SWM MTR with age, including: (1) inverted U-shaped trajectories of SWM MTR with age in the rostral middle frontal, medial temporal, and temporoparietal regions, which suggests myelination and protracted maturation of SWM till age 40–50 years and accelerating demyelination at age 60 years and beyond, (2) linear decline of SWM MTR with age in the middle and superior temporal, and pericalcarine areas, which may be interpreted as early maturation and less acceleration in age-related degeneration of SWM, and (3) no significant changes in SWM MTR in the primary motor (precentral), somatosensory (postcentral), auditory (Hechl's gyri) regions, which indicates early maturation and resistance to age-related deterioration of SWM.

SWM MTR in the rostral middle frontal, medial temporal (e.g., parahippocampus), and temporoparietal (e.g., supramarginal) regions followed inverted U-shaped trajectories with age. In these regions, SWM MTR increased slowly to 40 years of age, reached a plateau, and remained relatively stable during age 40–50 years before declining precipitously at age 60 years and beyond. In line with our observations, other studies reported similar inverted U-shaped patterns of change in WM volume ratio (i.e., the ratio of WM volume to total intracranial volume) and microstructure during normal aging [Bartzokis et al., 2001, 2012; Raz et al., 2010; Imperati et al., 2011; Kochunov et al., 2011; Taki et al., 2011; Chen

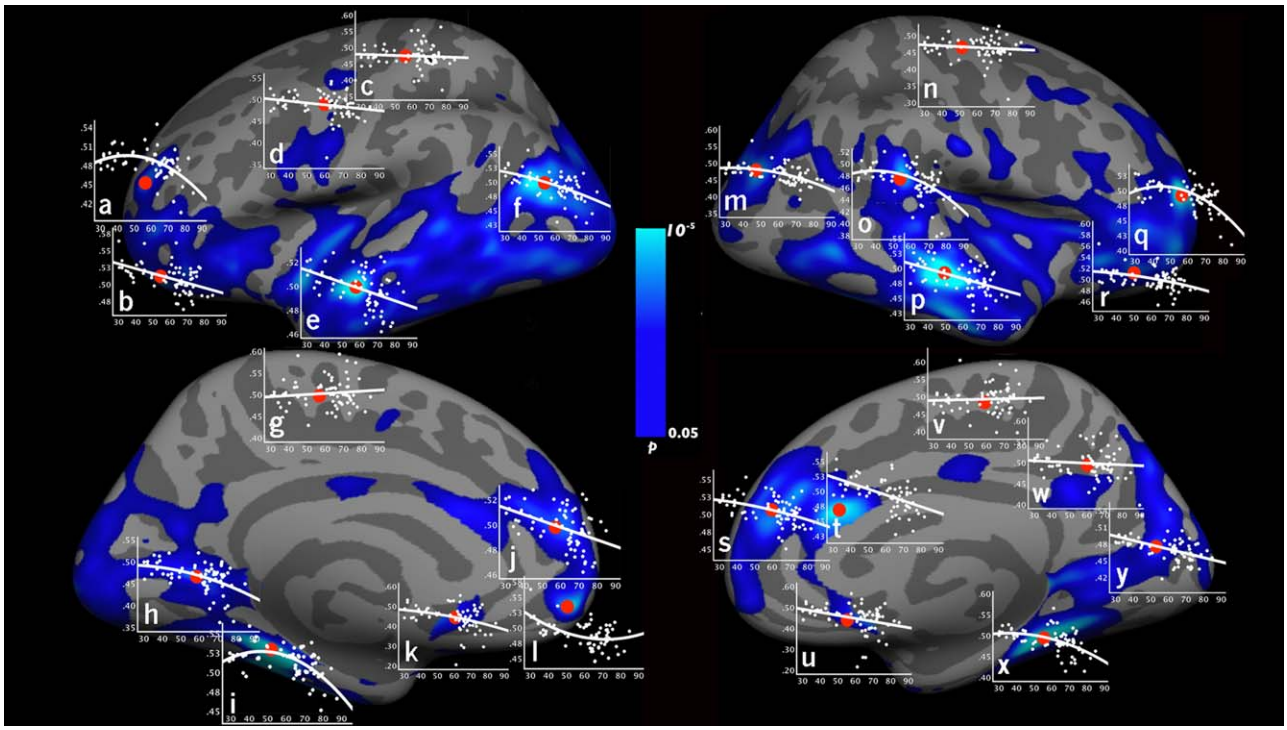

Figure 3.

Scatterplots of SWM MTR and age (graphs a–y) are shown at representative SWM vertices at different anatomical locations (as marked in red dots). The graphs were plotted with age on the x-axis (age range: 30–85 years) and SWM MTR on the y-axis. Left hemisphere: (a) rostral middle frontal, (b) lateral orbitofrontal, (c) postcentral, (d) precentral, (e) superior temporal, (f) inferior parietal, (g) paracentral, (h) lingual, (i) parahippocampus, (j) medial superior frontal, (k) rostral anterior cingulate, and (l) medial orbitofrontal. Right hemisphere: (m) inferior parietal, (n) precentral, (o) supramarginal, (p) middle temporal, (q) rostral middle frontal, (r) lateral orbitofrontal, (s) medial superior frontal, (t) caudal anterior cingulate, (u) rostral anterior cingulate, (v) paracentral, (w) precuneus, (x) parahippocampus, and (y) pericalcarine. Depending on the "goodness of fit" r^2, the curves in the graphs represent linear or quadratic line fittings. [Color figure can be viewed in the online issue, which is available at wileyonlinelibrary.com.]

et al., 2013]. Using a longitudinal design of over 6 years, Taki and colleagues showed that the WM ratio increased until around 50 years old before starting to decrease, following an inverted U-shaped curve [Taki et al., 2011]. Further, DTI-based studies also reported inverted U-shaped trajectories of WM microstructural changes with age [Imperati et al., 2011; Kochunov et al., 2011; Bartzokis et al., 2012; Chen et al., 2013]. Chen et al. demonstrated that in both humans and chimpanzees, the FA of regional and global WM exhibited a quadratic (inverted U-shaped) relationship with age [Chen et al., 2013]. Phillips et al. reported similar age-related changes in FA and RD in the middle frontal and temporoparietal (including supramarginal and angular) regions, but not in parahippocampus in healthy participants within a similar age range as those recruited in the present study [Phillips et al., 2013]. Consistent with these findings, the present study contributes that SWM MTR in above regions also follows inverted U-shaped developmental trajectories from young adulthood to old age.

SWM MTR in several regions (e.g., the middle and superior temporal [Fig. 3p,e] and the pericalcarine [Fig. 3y] regions) linearly declined with age. Similar linear changes of the microstructural measures of SWM with age were also reported in [Phillips et al., 2013]. Specifically, Phillips et al. [2013] demonstrated that SWM FA decreased linearly with age in the superior and middle temporal regions, accompanied by complementary increase of SWM RD in these regions. One possible explanation is that the SWM in these regions may mature earlier (e.g., before 30 years old) and have earlier onsets but less acceleration of MTR decline with age. With the limited age range of 30–85 years, the current study might not be able to capture increasing SWM MTR in these regions, but only characterized the linear decline of SWM MTR with age. Future work is needed to include younger individuals (i.e., <30 years of age) to verify this explanation.

MT imaging has been utilized to monitor changes in myelin integrity during normal brain development

[Engelbrecht et al., 1998] and aging [Silver et al., 1997], as well as disease progression [Horsfield et al., 2003; Fox et al., 2005; Zaaraoui et al., 2008]. Animal and human studies of multiple sclerosis have shown that brain regions with low MTR are accompanied by considerable myelin loss, and there is a significant correlation between MTR and the level of demyelination [Dousset et al., 1992; Brochet and Dousset, 1998; Schmierer et al., 2004], suggesting MTR as a marker of myelin integrity. Further, using an animal model of experimental chronic cerebral hypoperfusion to mimic age-related WM alterations, Holland et al. demonstrated that MTR is a sensitive marker of myelin damages and is capable of detecting diffuse and subtle biophysical changes in myelin during brain aging [Holland et al., 2011]. Because MTR is proportional to the macromolecular protein pools in WM (i.e., myelin), increased MTR in WM in developing brains is attributed to myelination [Barkovich, 2000; van Buchem et al., 2001], whereas reduced MTR in WM is attributed to myelin abnormalities, especially myelin loss or demyelination as seen in neurodegenerative brains [Silver et al., 1997].

As a sensitive marker of myelin integrity, divergent trajectories of SWM MTR with age (i.e., SWM MTR peaks or decreases at different ages or rates) suggest that myelin change (such as myelination, myelin loss or demyelination) in SWM occurs at varying paces across the cerebral cortex. Specifically, myelin in SWM regions including the rostral middle frontal, medial temporal and temporoparietal junction regions follows inverted U-shaped trajectories with age, with continuing myelination and relatively protracted maturation till age 40–50 years, and accelerating demyelination at age 60 years and beyond. In contrast, the primary motor (precentral), somatosensory (postcentral) and auditory (Hechl's gyri) regions do not show age-related deterioration in SWM. In line with our observations, minimal age-related changes of SWM FA and RD were reported in the precentral and postcentral areas [Phillips et al., 2013]. These converging findings suggest myelin integrity in these SWM regions is largely maintained in normal aging.

Regionally varying susceptibility to myelin degradation in SWM during normal aging may relate to different myelination mechanisms and fiber profiles in the regions. In the central nervous system, oligodendrocytes produce and maintain myelin [Fünfschilling et al., 2012], and they are markedly heterogeneous through the protracted developmental process of SWM. Compared with oligodendrocytes in the early-myelinating SWM regions (e.g., the primary somatosensory and motor regions), oligodendrocytes in the late-maturing SWM regions (e.g., parahippocampus) produce thinner myelin, ensheathe more axons of smaller diameters in diverse directions, have slower rate of turnover and are less efficient for myelin repair [Wood and Bunge, 1984; Bartzokis, 2004]. The characteristics of late-differentiating oligodendrocytes may render the late-myelinating SWM regions more vulnerable to age-related degenerative processes, with accelerating decline after age 60 years. In contrast, early-differentiating oligodendrocytes produce thicker myelin, sheathe fewer axons of larger diameters, and have more rapid myelin turnover as well as a better ability for myelin repair [Wood and Bunge, 1984; Bartzokis, 2004], which may lead to resistance to age-related deterioration in the early-myelinating SWM regions (e.g., the primary somatosensory and motor regions). Stereological studies demonstrated that thousands of kilometers of thin fibers were lost but essentially all the thick fibers were retained during normal aging [Tang et al., 1997; Pakkenberg et al., 2003], suggesting thin fibers are more prone to age-related degeneration. It is possible that varying properties of oligodendrocytes may contribute to the regionally varying vulnerability of SWM myelin. However, future work is needed to combine imaging and histological methods to directly link properties of oligodendrocytes with vulnerability of SWM myelin during aging.

The heterogeneous relationships between SWM MTR and age across the cortex may provide an explanation for inconsistent findings of previous MT-based studies on WM aging. Armstrong et al. reported significant positive correlation between MTR and age [Armstrong et al., 2004], which deviated from reports of negative correlations [Silver et al., 1997; Hofman et al., 1999; Ge et al., 2002] or no age effect on MTR [Mehta et al., 1995] in regional or global WM. These studies used ROI-based or global histogram-based approaches, which averaged MTR changes in large areas and might miss sub-regional variations. In contrast, VBSS can detect MTR changes in SWM with a finer spatial resolution. Further, these studies only examined linear relationships between MTR and age, which might overshadow possible quadratic relationships in some SWM regions.

We evaluated the linear and quadratic effects of age on cortical thickness as well (see Supporting Information Fig. 1), which aligned well with the literature findings. For example, in the present study, significant cortical thinning with age was observed in the inferior frontal gyrus and superior and middle temporal gyrus, which were among regions with the strongest age effects across multiple samples [Fjell et al., 2009]. Significant age effects were also found in fusiform and pericalarine, which were previously found to be very prone to age effects [Fjell et al., 2009]. Our data also demonstrated significant decrease of cortical thickness with age in the precentral gyrus, which was found in some samples [Salat et al., 2004] but not in others [Fjell et al., 2009]. Comparing Figure 2 and Supporting Information Figure 1, there is no substantial spatial overlap in the age effects between SWM MTR and cortical thickness. For example, age-related decrease of SWM MTR was observed in a large frontal SWM area encompassing the orbitofrontal, inferior frontal, rostral middle frontal, and superior frontal regions, while change in cortical thickness was observed only in smaller areas of left

orbitofrontal and right inferior frontal regions. In addition, cortical thickness of the primary motor region decreased linearly with age, but the SWM MTR of the same region did not demonstrate an age-related decline. Distinct age effects on SWM and cortical GM suggest that the age-related changes of SWM MTR in the present study were not due to cortical atrophy but reflected alterations of SWM myelin with age.

Several limitations of the present study should be considered. Firstly, we used MTR to measure the myelin status in SWM, which is based on a two-pool model for quantitative interpretation of MT effects [Henkelman et al., 1993]. More complex biophysical models have been proposed and may provide additional insight into the underlying mechanisms of MT effects. Secondly, while MTR is a valid and useful measure for quantitation of MT effects, the actual amount of magnetization transfer depends on two competing processes: the exchange of magnetization between tissue compartments and the recovery of magnetization from T_1 relaxation within each tissue compartment. As a result, MTR may depend on tissue type and MT pulse sequences and parameters [Henkelman et al., 2001]. Such variations make it difficult to compare results across studies and may have also contributed to the inconsistent findings of MTR in WM aging in the literature. Thirdly, animal and human postmortem MT and histopathological studies have shown that MTR is a sensitive marker of semisolid constituents of biological tissue and primarily reflects myelin in the white matter [Deloire-Grassin et al., 2000; Levesque and Pike, 2009]. However, it was previously reported that MTR was also correlated with the change in water content due to inflammation and edema in pathological tissue [Vavasour et al., 2011]. Contradictorily, some studies showed that the changes of T_1 due to edema and inflammation had minimal effect on MTR in acute lesions [Giacomini et al., 2009; Vavasour et al., 2011] and the effects of edema on MTR in nonacute lesions were only moderate [Ropele et al., 2000]. These contradictory findings warrant caution when associating MTR with myelin in the presence of edema and/or inflammation. Whether in the presence or absence of edema and/or inflammation, there were consistent correlations between MTR and myelin integrity in the above studies. This study only involved healthy participants, in which edema and inflammation in brain tissues were negligible; therefore the MTR measured in the present study primarily reflected the integrity of myelin in SWM.

Other limitations of the present study are included below. Partial volume effects can influence the calculation of SWM MTR. To reduce the partial volume effects, we sampled and averaged SWM MTR from 1 up to 5 mm from the GM/WM boundary. A cross-sectional instead of longitudinal design was used in this study. The cross-sectional design evaluates age-related changes through correlations, which is inherently vulnerable to intersubject variance and cohort effects. The present study has a relatively modest sample size ($N = 66$), which may not have sufficient power to detect subtle myelin changes in some SWM areas. Future studies with more participants and longitudinal designs will be valuable to further confirm our findings.

ACKNOWLEDGMENTS

The authors thank Dr. Peter van Zijl and Joseph S. Gillen (Johns Hopkins University) for the MT sequence, which was developed by the support of the National Institute of Biomedical Imaging and Bioengineering resource grant P41 EB015909.

REFERENCES

Armstrong CL, Traipe E, Hunter JV, Haselgrove JC, Ledakis GE, Tallent EM, Shera D, van Buchem MA (2004): Age-related, regional, hemispheric, and medial-lateral differences in myelin integrity in vivo in the normal adult brain. Am J Neuroradiol 25:977–984.

Barkovich AJ (2000): Concepts of myelin and myelination in neuroradiology. AJNR Am J Neuroradiol 21:1099–1109.

Bartzokis G (2004): Age-related myelin breakdown: A developmental model of cognitive decline and Alzheimer's disease. Neurobiol Aging 25:5–18.

Bartzokis G, Beckson M, Lu PH, Nuechterlein KH, Edwards N, Mintz J (2001): Age-related changes in frontal and temporal lobe volumes in men: A magnetic resonance imaging study. Arch Gen Psychiatry 58:461–465.

Bartzokis G, Lu PH, Heydari P, Couvrette A, Lee GJ, Kalashyan G, Freeman F, Grinstead JW, Villablanca P, Finn JP (2012): Multimodal magnetic resonance imaging assessment of white matter aging trajectories over the lifespan of healthy individuals. Biol Psychiatry 72:1026–1034.

Brochet B, Dousset V (1998): Pathological correlates of magnetization transfer imaging abnormalities in animal models and humans with multiple sclerosis. Neurology 53:S12–S17.

Cercignani M, Alexander DC (2006): Optimal acquisition schemes for in vivo quantitative magnetization transfer MRI. Magn Reson Med 56:803–810.

Chen JT, Collins DL, Atkins HL, Freedman MS, Arnold DL (2008): Magnetization transfer ratio evolution with demyelination and remyelination in multiple sclerosis lesions. Ann Neurol 63:254–262.

Chen X, Errangi B, Li L, Glasser MF, Westlye LT, Fjell AM, Walhovd KB, Hu X, Herndon JG, Preuss TM (2013): Brain aging in humans, chimpanzees (*Pan troglodytes*), and rhesus macaques (*Macaca mulatta*): Magnetic resonance imaging studies of macro-and microstructural changes. Neurobiol Aging 34: 2248–2260.

Collins DL, Neelin P, Peters TM, Evans AC (1994): Automatic 3D intersubject registration of MR volumetric data in standardized Talairach space. J Comput Assisted Tomogr 18:192–205.

Dale AM, Fischl B, Sereno MI (1999): Cortical surface-based analysis: I. Segmentation and surface reconstruction. Neuroimage 9: 179–194.

Davis SW, Dennis NA, Buchler NG, White LE, Madden DJ, Cabeza R (2009): Assessing the effects of age on long white matter tracts using diffusion tensor tractography. Neuroimage 46:530–541.

Deloire-Grassin MS, Brochet B, Quesson B, Delalande C, Dousset V, Canioni P, Petry KG (2000): In vivo evaluation of

remyelination in rat brain by magnetization transfer imaging. J Neurol Sci 178:10–16.
Dousset V, Grossman RI, Ramer KN, Schnall MD, Young LH, Gonzalez-Scarano F, Lavi E, Cohen JA (1992): Experimental allergic encephalomyelitis and multiple sclerosis: Lesion characterization with magnetization transfer imaging. Radiology 182:483–491.
Engelbrecht V, Rassek M, Preiss S, Wald C, M+ldder U (1998): Age-dependent changes in magnetization transfer contrast of white matter in the pediatric brain. Am J Neuroradiol 19:1923–1929.
Fazekas F, Kleinert R, Offenbacher H, Schmidt R, Kleinert G, Payer F, Radner H, Lechner H (1993): Pathologic correlates of incidental MRI white matter signal hyperintensities. Neurology 43:1683
Fazekas F, Ropele S, Enzinger C, Gorani F, Seewann A, Petrovic K, Schmidt R (2005): MTI of white matter hyperintensities. Brain 128:2926–2932.
Fischl B, Sereno MI, Dale AM (1999b): Cortical surface-based analysis: II: Inflation, flattening, and a surface-based coordinate system. Neuroimage 9:195–207.
Fischl B, Sereno MI, Tootell RB, Dale AM (1999a): High-resolution intersubject averaging and a coordinate system for the cortical surface. Human Brain Mapping 8:272–284.
Fjell AM, Westlye LT, Amlien I, Espeseth T, Reinvang I, Raz N, Agartz I, Salat DH, Greve DN, Fischl B (2009): High consistency of regional cortical thinning in aging across multiple samples. Cereb Cortex 19:2001–2012.
Fox RJ, Fisher E, Tkach J, Lee JC, Cohen JA, Rudick RA (2005): Brain atrophy and magnetization transfer ratio following methylprednisolone in multiple sclerosis: Short-term changes and long-term implications. Mult Scler 11:140–145.
Fünfschilling U, Supplie LM, Mahad D, Boretius S, Saab AS, Edgar J, Brinkmann BG, Kassmann CM, Tzvetanova ID, M+lbius W (2012): Glycolytic oligodendrocytes maintain myelin and long-term axonal integrity. Nature 485:517–521.
Ge Y, Grossman RI, Babb JS, Rabin ML, Mannon LJ, Kolson DL (2002): Age-related total gray matter and white matter changes in normal adult brain. Part II: Quantitative magnetization transfer ratio histogram analysis. Am J Neuroradiol 23:1334–1341.
Giacomini PS, Levesque IR, Ribeiro L, Narayanan S, Francis SJ, Pike GB, Arnold DL (2009): Measuring demyelination and remyelination in acute multiple sclerosis lesion voxels. Arch Neurol 66:375–381.
Hagler DJ Jr, Saygin AP, Sereno MI (2006): Smoothing and cluster thresholding for cortical surface-based group analysis of fMRI data. Neuroimage 33:1093–1103.
Henkelman RM, Huang X, Xiang QS, Stanisz GJ, Swanson SD, Bronskill MJ (1993): Quantitative interpretation of magnetization transfer. Magn Reson Med 29:759–766.
Henkelman RM, Stanisz GJ, Graham SJ (2001): Magnetization transfer in MRI: A review. NMR Biomed 14:57–64.
Hofman PAM, Kemerink GJ, Jolles J, Wilmink JT (1999): Quantitative analysis of magnetization transfer images of the brain: Effect of closed head injury, age and sex on white matter. Magn Reson Med 42:803–806.
Holland PR, Bastin ME, Jansen MA, Merrifield GD, Coltman RB, Scott F, Nowers H, Khallout K, Marshall I, Wardlaw JM (2011): MRI is a sensitive marker of subtle white matter pathology in hypoperfused mice. Neurobiol Aging 32:2325. 23e1
Horsfield MA, Barker GJ, Barkhof F, Miller DH, Thompson AJ, Filippi M (2003): Guidelines for using quantitative magnetization transfer magnetic resonance imaging for monitoring treatment of multiple sclerosis. J Magn Reson Imaging 17:389–397.
Imperati D, Colcombe S, Kelly C, Di Martino A, Zhou J, Castellanos FX, Milham MP (2011): Differential development of human brain white matter tracts. PLoS One 6:e23437
Jernigan TL, Archibald SL, Fennema-Notestine C, Gamst AC, Stout JC, Bonner J, Hesselink JR (2001): Effects of age on tissues and regions of the cerebrum and cerebellum. Neurobiol Aging 22:581–594.
Kim KW, MacFall JR, Payne ME (2008): Classification of white matter lesions on magnetic resonance imaging in elderly persons. Biol. Psychiatry 64:273–280.
Kochunov P, Glahn DC, Lancaster J, Thompson PM, Kochunov V, Rogers B, Fox P, Blangero J, Williamson DE (2011): Fractional anisotropy of cerebral white matter and thickness of cortical gray matter across the lifespan. Neuroimage 58:41–49.
Kumar A, Gupta R, Thomas A, Ajilore O, Hellemann G (2009): Focal subcortical biophysical abnormalities in patients diagnosed with type 2 diabetes and depression. Arch Gen Psychiatry 66:324–330.
Levesque IR, Pike GB (2009): Characterizing healthy and diseased white matter using quantitative magnetization transfer and multicomponent T(2) relaxometry: A unified view via a four-pool model. Magn Reson Med 62:1487–1496.
Longstreth WT, Manolio TA, Arnold A, Burke GL, Bryan N, Jungreis CA, Enright PL, O'Leary D, Fried L (1996): Clinical correlates of white matter findings on cranial magnetic resonance imaging of 3301 elderly people The Cardiovascular Health Study. Stroke 27:1274–1282.
Maricich SM, Azizi P, Jones JY, Morriss MC, Hunter JV, Smith EO, Miller G (2007): Myelination as assessed by conventional MR imaging is normal in young children with idiopathic developmental delay. AJNR Am J Neuroradiol 28:1602–1605.
Mehta RC, Pike GB, Enzmann DR (1995): Magnetization transfer MR of the normal adult brain. Am J Neuroradiol 16:2085–2091.
Mehta RC, Pike GB, Enzmann DR (1996): Magnetization transfer magnetic resonance imaging: A clinical review. Topics Magn Reson Imaging 8:214–230.
Meynert T (1872): In: Stricker S, editor. Handbuch der Lehre von den Geweben des Menschen und der Thiere, Vol. 1. Leipzig: W. Engelmann. pp 694–808.
Pakkenberg B, Pelvig D, Marner L, Bundgaard MJ, Gundersen HJ, Nyengaard JR, Regeur L (2003): Aging and the human neocortex. Exp Gerontol 38:95–99.
Phillips OR, Clark KA, Luders E, Azhir R, Joshi SH, Woods RP, Mazziotta JC, Toga AW, Narr KL (2013): Superficial white matter: Effects of age, sex, and hemisphere. Brain Connect 3:146–159.
Raz N, Ghisletta P, Rodrigue KM, Kennedy KM, Lindenberger U (2010): Trajectories of brain aging in middle-aged and older adults: Regional and individual differences. Neuroimage 51:501–511.
Raz N, Lindenberger U, Rodrigue KM, Kennedy KM, Head D, Williamson A, Dahle C, Gerstorf D, Acker JD (2005): Regional brain changes in aging healthy adults: General trends, individual differences and modifiers. Cereb Cortex 15:1676–1689.
Reiser MF, Semmler W, Hricak H (2008): Magnetic resonance tomography. Springer-Verlag, Berlin Heidelberg.
Schüz A, Chaimow D, Liewald D, Dortenman M (2006): Quantitative aspects of corticocortical connections: a tracer study in the mouse. Cereb Cortex 16:1474–1486.
Schmierer K, Scaravilli F, Altmann DR, Barker GJ, Miller DH (2004): Magnetization transfer ratio and myelin in postmortem multiple sclerosis brain. Ann Neurol 56:407–415.

Silver NC, Barker GJ, MacManus DG, Tofts PS, Miller DH (1997): Magnetisation transfer ratio of normal brain white matter: A normative database spanning four decades of life. J Neurol Neurosurg Psychiatry 62:223–228.

Smith SA, Farrell JA, Jones CK, Reich DS, Calabresi PA, van Zijl PC (2006): Pulsed magnetization transfer imaging with body coil transmission at 3 Tesla: Feasibility and application. Magn Reson Med 56:866–875.

Spilt A, Goekoop R, Westendorp RGJ, Blauw GJ, de Craen AJM, van Buchem MA (2006): Not all age-related white matter hyperintensities are the same: A magnetization transfer imaging study. Am J Neuroradiol 27:1964–1968.

Stadlbauer A, Salomonowitz E, Strunk G, Hammen T, Ganslandt O (2008): Age-related degradation in the central nervous system: Assessment with diffusion-tensor imaging and quantitative fiber tracking 1. Radiology 247:179–188.

Stanisz GJ, Kecojevic A, Bronskill MJ, Henkelman RM (1999): Characterizing white matter with magnetization transfer and T2. Magn Reson Med 42:1128–1136.

Sullivan EV, Adalsteinsson E, Hedehus M, Ju C, Moseley M, Lim KO, Pfefferbaum A (2001): Equivalent disruption of regional white matter microstructure in ageing healthy men and women. Neuroreport 12:99–104.

Talairach J, Tournoux P (1988): Co-planar stereotaxic atlas of the human brain: 3-Dimensional proportional system. An approach to cerebral imaging. Thieme Medical Publishers, New York.

Taki Y, Kinomura S, Sato K, Goto R, Kawashima R, Fukuda H (2011): A longitudinal study of gray matter volume decline with age and modifying factors. Neurobiology of Aging 32:907–915.

Tamnes CK, +ÿstby Y, Fjell AM, Westlye LT, Due-T++nnessen P, Walhovd KB (2010): Brain maturation in adolescence and young adulthood: Regional age-related changes in cortical thickness and white matter volume and microstructure. Cereb Cortex 20:534–548.

van Buchem MA, Steens SC, Vrooman HA, Zwinderman AH, McGowan JC, Rassek M, Engelbrecht V (2001): Global estimation of myelination in the developing brain on the basis of magnetization transfer imaging: A preliminary study. Am J Neuroradiol 22:762–766.

Wolff SD, Balaban RS (1989): Magnetization transfer contrast (MTC) and tissue water proton relaxation in vivo. Magn Reson Med 10:135–144.

Wood P, Bunge RP (1984): The biology of the oligodendrocyte. In: Oligodendroglia. Advances in Neurochemistry, Vol. 5. (Norton WT, ed.) Springer, New York. pp 1–46.

Wu M, Lu LH, Lowes A, Yang S, Passarotti AM, Zhou XJ, Pavuluri MN (2014): Development of superficial white matter and its structural interplay with cortical gray matter in children and adolescents. Hum Brain Mapp 35:2806–2816.

Tang Y, Nyengaard JR, Pakkenberg B, Gundersen HJG (1997): Age-induced white matter changes in the human brain: A stereological investigation. Neurobiol Aging 18:609–615.

Salat DH, Buckner RL, Snyder AZ, Greve DN, Desikan RS, Busa E, Morris JC, Dale AM, Fischl B (2004): Thinning of the cerebral cortex in aging. Cereb Cortex 14:721–730.

Vavasour IM, Laule C, Li DK, Traboulsee AL, Mackay AL (2011): Is the magnetization transfer ratio a marker for myelin in multiple sclerosis? J Magn Reson Imaging 33:713–718.

Ropele S, Strasser-Fuchs S, Augustin M, Stollberger R, Enzinger C, Hartung HP, Fazekas F (2000): A comparison of magnetization transfer ratio, magnetization transfer rate, and the native relaxation time of water protons related to relapsing-remitting multiple sclerosis. AJNR Am J Neuroradiol 21:1885–1891.

Ylikoski A, Erkinjuntti T, Raininko R, Sarna S, Sulkava R, Tilvis R (1995): White matter hyperintensities on MRI in the neurologically nondiseased elderly Analysis of cohorts of consecutive subjects aged 55 to 85 years living at home. Stroke 26:1171–1177.

Zaaraoui W, Deloire M, Merle M, Girard C, Raffard G, Biran M, Inglese M, Petry KG, Gonen O, Brochet B, Franconi JM, Dousset V (2008): Monitoring demyelination and remyelination by magnetization transfer imaging in the mouse brain at 9.4 T. Magma 21:357–362.